IEICE TRANS. ELECTRON., VOL.E87–C, NO.5 MAY 2004

PAPER Special Section on Measurement Technologies for Microwave Materials, Devices and Circuits

Hybrid MOM-Immittance Approach for Full-Wave Characterization of Printed Strips and Slots in Layered Waveguide and Its Applications

Rakhesh Singh KSHETRIMAYUM[†a)], ***Nonmember and*** **Lei ZHU**[†b)], ***Member***

SUMMARY A hybrid method-of-moments (MoM) and immittance approach for efficient and accurate analysis of printed slots and strips of arbitrary shape in layered waveguide for various applications has been proposed. An impedance-type MoM is formulated from the electric field integral equation (EFIE) for printed strip case and an admittance-type MoM is formulated from the magnetic field integral equation (MFIE) for the printed slot case, using the Galerkin's technique. Immittance approach has been used to calculate spectral dyadic Green's functions for the layered waveguide. For efficient analysis of large and complex structures, equivalent circuit parameters of a block are first extracted and complete structure is analyzed through cascaded ABCD matrices. The equivalent circuit characterization of printed strip and slot in layered waveguide has been done for the first time. Finite periodic structure loaded with printed strips has been investigated and it shows the electromagnetic bandgap (EBG) behavior. The electromagnetic (EM) program hence developed is checked for its numerical accuracy and efficiency with results generated with High-frequency structure simulator (HFSS) and shows good performance.

key words: *printed strips and slots, method of moments, equivalent circuits, bandpass filter, periodic structures*

1. Introduction

Printed strips and slots are basic building blocks for many waveguide based structures and they are printed on a dielectric layer. Commonly used waveguide elements like inductive and capacitive strips, diaphragms, iris, etc. [1]–[4] are special cases of printed strips and slots where the thickness of the dielectric layer is reduced to zero. An excellent literature on waveguide filters, impedance matching and coupling structures is given in [5] and equivalent circuits of many common waveguide elements are listed in [6], [7] using variational techniques. It is our objective to extract the equivalent circuits of printed strips and slots in layered waveguide using method-of-moments (MoM) so that cascaded network based synthesis design using such structures can be implemented easily. Planar strips and slots also have been studied for spatial power combining applications in [8].

In this paper, the admittance-type and impedance-type MoM are formulated respectively for printed slot and strip. The immitance approach as described in [9], [10] has been used to calculate the spectral dyadic Green's functions for the multilayered waveguide structures with printed strips and/or printed slots. The electromagnetic (EM) program hence developed has been checked for its accuracy for various waveguide elements with the High-frequency structure simulator (HFSS) results and shows good agreement. Then, equivalent circuit parameters of printed strip and slot in layered waveguide have been extracted. Finite periodic structure loaded with printed strip has also been investigated. Finally a compact and broadband band pass filter has been designed using our proposed method and compared with HFSS.

Manuscript received September 2, 2003.
Manuscript revised December 12, 2003.

[†]The authors are with the School of Electrical & Electronic Engineering, Nanyang Technological University, Nanyang Avenue, 639798 Singapore.
a) E-mail: rakhesh@pmail.ntu.edu.sg
b) E-mail: ezhul@ntu.edu.sg

2. Theoretical Formulation

2.1 Impedance-Type MoM Formulation

Figure 1 depicts the three-dimensional geometry of waveguide discontinuity under consideration. The layered waveguide can be divided into three regions, region I of relative permittivity ϵ_1, region II of relative permittivity ϵ_2 and region III of relative permittivity ϵ_3. The printed strip of any arbitrary shape and size is located at the interface #1. The thickness of the dielectric substrate layer i.e. region II is denoted by h. The electromagnetic waves incident from region I are scattered at the interface #1 and transmitted through region II to region III. The electric field integral equation (EFIE) can be obtained from the boundary condition on the tangential components of the total electric field, which consists of incident and scattered electric field, on the printed strip is zero.

$$\hat{z} \times \mathbf{E}^{inc}(\mathbf{r}) + \hat{z} \times \int_{strip} \bar{\mathbf{G}}_{EJ}(\mathbf{r}', \mathbf{r}) \cdot \mathbf{J}(\mathbf{r}') d\mathbf{S}' = 0 \qquad (1)$$

In the above equation, the scattered electric field is expressed in terms of electric dyadic Green's functions and

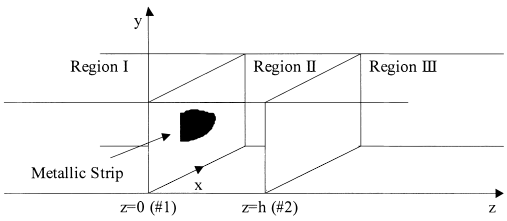

Fig. 1 Geometry of printed strip in layered waveguide.

electric current density over the printed strip. After discretizing the electric current density over the strip by using appropriate basis functions and applying Galerkin's method, we can transform the EFIE into matrix systems of linear equations. Using Fourier transform technique and after doing some mathematical manipulations, we have arrived at a simple expression for impedance-type MoM matrix equation.

$$\begin{bmatrix} [Z_{xx}] & [Z_{xy}] \\ [Z_{yx}] & [Z_{yy}] \end{bmatrix} \begin{bmatrix} [I_x] \\ [I_y] \end{bmatrix} = \begin{bmatrix} [V_x] \\ [V_y] \end{bmatrix} \tag{2}$$

where the elements of each sub-matrices are expressed as

$$z_{xx}(m,n) = -\sum_{m=0}^{M+1}\sum_{n=0}^{N+1} \tilde{B}_x(k_{xm},k_{yn})\tilde{G}_{EJ}^{xx}(k_{xm},k_{yn})\tilde{T}_x^*(k_{xm},k_{yn})$$

$$z_{xy}(m,n) = -\sum_{m=0}^{M+1}\sum_{n=0}^{N+1} \tilde{B}_x(k_{xm},k_{yn})\tilde{G}_{EJ}^{xy}(k_{xm},k_{yn})\tilde{T}_y^*(k_{xm},k_{yn})$$

$$z_{yx}(m,n) = -\sum_{m=0}^{M+1}\sum_{n=0}^{N+1} \tilde{B}_y(k_{xm},k_{yn})\tilde{G}_{EJ}^{yx}(k_{xm},k_{yn})\tilde{T}_x^*(k_{xm},k_{yn})$$

$$z_{yy}(m,n) = -\sum_{m=0}^{M+1}\sum_{n=0}^{N+1} \tilde{B}_y(k_{xm},k_{yn})\tilde{G}_{EJ}^{yy}(k_{xm},k_{yn})\tilde{T}_y^*(k_{xm},k_{yn})$$

$$V_x = \iint_{strip} T_x^*(x,y)E_x^{inc}(x,y)\,dx\,dy$$

$$V_y = \iint_{strip} T_y^*(x,y)E_y^{inc}(x,y)\,dx\,dy$$

In the above equation, $B_x(x,y)$, $B_y(x,y)$ are the x- and y-directed basis functions while $T_x(x,y)$, $T_y(x,y)$ are the x- and y-directed testing functions. In Galerkin's method, basis functions are chosen the same as the testing functions which is composed of piecewise sinusoidal functions along current direction and pulse functions in the transverse direction. $\tilde{B}_x(x,y)$, $\tilde{B}_y(x,y)$ are the Fourier transform pairs of x- and y-directed basis functions while $\tilde{T}_x^*(x,y)$, $\tilde{T}_y^*(x,y)$ are the complex conjugate of the Fourier transform pairs of x- and y-directed testing functions. The sub-matrices $[V_x]$ and $[V_y]$ refer to the x- and y-directed testing of the incident electric field. We have considered the case for the dominant TE_{10} mode only here. By choosing incident mode for other higher modes, we can also do the multimode full-wave analysis of such kinds of structures. $[I_x]$ and $[I_y]$ sub-matrices are respectively the unknown electric current expansion coefficients associated with x-directed and y-directed basis function. For the printed strip inside layered waveguide of geometry shown in Fig. 1, the equivalent transverse electric (TE) and transverse magnetic (TM) transmission line model [9], [10] using the immittance approach is as shown in Fig. 2.

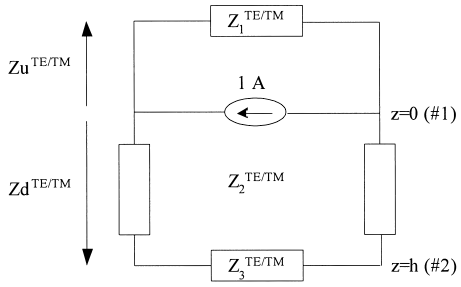

Fig. 2 Equivalent TE/TM transmission line model for transverse electric point source excitation in waveguide.

In Fig. 2, Z_1^{TE}, Z_2^{TE} and Z_3^{TE} are respectively the wave impedances of TE mode in region I, region II, and region III of the waveguide. Similarly, Z_1^{TM}, Z_2^{TM} and Z_3^{TM} are respectively the wave impedances of TM mode in region I, region II, and region III of the waveguide. The equivalent impedance looking up from the interface #1 for the TE and TM mode cases are

$$Z_u^{TE} = Z_1^{TE}; \quad Z_u^{TM} = Z_1^{TM} \tag{3}$$

Whereas the equivalent impedance looking down from the interface #1 for the TE and TM mode cases are

$$\begin{aligned} Z_d^{TE} &= Z_3^{TE}\frac{Z_2^{TE} + jZ_3^{TE}\tanh(\gamma_2 h)}{Z_3^{TE} + jZ_2^{TE}\tanh(\gamma_2 h)} \\ Z_d^{TM} &= Z_3^{TM}\frac{Z_2^{TM} + jZ_3^{TM}\tanh(\gamma_2 h)}{Z_3^{TM} + jZ_2^{TM}\tanh(\gamma_2 h)} \end{aligned} \tag{4}$$

In the above equation, γ_2 is the propagation constant of EM wave in the waveguide region II. Let us denote the equivalent impedance by Z^{TE} for TE mode then $Z^{TE} = Z_u^{TE} \| Z_d^{TE}$ due to the shunt combination of Z_u^{TE} and Z_d^{TE}; similarly let us denote the equivalent impedance for TM mode Z^{TM} then $Z^{TM} = Z_u^{TM} \| Z_d^{TM}$. The electric dyadic Green's function in the spectral domain when the source and observation points are both at the interface #1 is

$$\begin{aligned} \tilde{\tilde{G}}_{EJ}^{11}(\mathbf{k}_t, z=0, z'=0) &= -V_1^{TE}(\mathbf{k}_t,0,0)(\hat{k}_t\times\hat{z})(\hat{k}_t\times\hat{z}) \\ &- V_1^{TM}(\mathbf{k}_t,0,0)(\hat{k}_t)(\hat{k}_t) \\ &= -Z^{TE}(\hat{k}_t\times\hat{z})(\hat{k}_t\times\hat{z}) - Z^{TM}(\hat{k}_t)(\hat{k}_t) \end{aligned} \tag{5}$$

The primed z coordinates represent the source locations whereas the unprimed z coordinates represent the observation point. V_1^{TE} and V_1^{TM} are the voltage across the interface #1 for TE and TM mode respectively. $\mathbf{k}_t$ is the transverse vector wave number and can be expressed as

$$\mathbf{k}_t = k_{xm}\hat{x} + k_{yn}\hat{y} = \left(\frac{m\pi}{a}\right)\hat{x} + \left(\frac{n\pi}{b}\right)\hat{y} = |\mathbf{k}_t|\hat{k} \tag{6}$$

where m and n are integers denoting the waveguide modes. Similarly, the electric dyadic Green's function when the source is at the interface #1 and observation point is at the interface #2 in the spectral domain is

$$\begin{aligned}
&\tilde{\tilde{G}}_{EJ}^{21}(\mathbf{k}_t, z=h, z'=0) \\
&\quad = -V_2^{TE}(\mathbf{k}_t, h, 0)(\hat{k}_t \times \hat{z})(\hat{k}_t \times \hat{z}) \\
&\qquad - V_2^{TM}(\mathbf{k}_t, h, 0)(\hat{k}_t)(\hat{k}_t) \\
&\quad = -\left\{ Z_3^{TE} \times \frac{Z^{TE}}{Z_d^{TE}} \right\} (\hat{k}_t \times \hat{z})(\hat{k}_t \times \hat{z}) \\
&\qquad - \left\{ Z_3^{TM} \times \frac{Z^{TM}}{Z_d^{TM}} \right\} (\hat{k}_t)(\hat{k}_t)
\end{aligned} \tag{7}$$

In the above equation, V_2^{TE} and V_2^{TM} are the voltage across the interface #2 for TE and TM mode respectively. The four components of the electric dyadic Green's function in the spectral domain of Eqs. (5) and (7) can be obtained as

$$\begin{aligned}
\tilde{G}_{EJ}^{xx}(k_{xm}, k_{yn}) &= -\frac{k_{xm}^2 Z^{TM} + k_{yn}^2 Z^{TE}}{k_{xm}^2 + k_{yn}^2} \\
\tilde{G}_{EJ}^{yy}(k_{xm}, k_{yn}) &= -\frac{k_{xm}^2 Z^{TE} + k_{yn}^2 Z^{TM}}{k_{xm}^2 + k_{yn}^2} \\
\tilde{G}_{EJ}^{xy/yx}(k_{xm}, k_{yn}) &= -\frac{k_{xm} k_{yn} (Z^{TM} - Z^{TE})}{k_{xm}^2 + k_{yn}^2}
\end{aligned} \tag{8}$$

2.2 Admittance-Type MoM Formulation

Figure 3 shows the three-dimensional geometry of waveguide discontinuity under consideration. The printed slot of any arbitrary shape and size is located at the interface #2. The magnetic field integral equation (MFIE) is obtained by enforcing boundary condition on the tangential components of the total magnetic field, which consists of incident and scattered magnetic field, on the printed slot is zero.

$$\hat{z} \times \mathbf{H}^{inc}(\mathbf{r}) + \hat{z} \times \int_{slot} \bar{\mathbf{G}}_{HM}(\mathbf{r}', \mathbf{r}) \cdot \mathbf{M}(\mathbf{r}') d\mathbf{S}' = 0 \tag{9}$$

In the above equation, the scattered magnetic field is expressed in terms of magnetic dyadic Green's functions and magnetic current density over the slot. After discretizing the magnetic current density over the slot by using appropriate basis functions and applying Galerkin's method, we get the admittance-type MoM matrix equation as follows

$$\begin{bmatrix} [Y_{xx}] & [Y_{xy}] \\ [Y_{yx}] & [Y_{yy}] \end{bmatrix} \begin{bmatrix} [V_x] \\ [V_y] \end{bmatrix} = \begin{bmatrix} [I_x] \\ [I_y] \end{bmatrix} \tag{10}$$

where the elements of each sub-matrices are expressed as

$$\begin{aligned}
&y_{xx}(m,n) \\
&\quad = -\sum_{m=0}^{M+1} \sum_{n=0}^{N+1} \tilde{B}_x(k_{xm}, k_{yn}) \tilde{G}_{HM}^{xx}(k_{xm}, k_{yn}) \tilde{T}_x^*(k_{xm}, k_{yn}) \\
&y_{xy}(m,n) \\
&\quad = -\sum_{m=0}^{M+1} \sum_{n=0}^{N+1} \tilde{B}_x(k_{xm}, k_{yn}) \tilde{G}_{HM}^{xy}(k_{xm}, k_{yn}) \tilde{T}_y^*(k_{xm}, k_{yn}) \\
&y_{yx}(m,n) \\
&\quad = -\sum_{m=0}^{M+1} \sum_{n=0}^{N+1} \tilde{B}_y(k_{xm}, k_{yn}) \tilde{G}_{HM}^{yx}(k_{xm}, k_{yn}) \tilde{T}_x^*(k_{xm}, k_{yn}) \\
&y_{yy}(m,n) \\
&\quad = -\sum_{m=0}^{M+1} \sum_{n=0}^{N+1} \tilde{B}_y(k_{xm}, k_{yn}) \tilde{G}_{HM}^{yy}(k_{xm}, k_{yn}) \tilde{T}_y^*(k_{xm}, k_{yn}) \\
&I_x = \iint_{strip} T_x^*(x,y) H_x^{inc}(x,y)\, dx\, dy \\
&I_y = \iint_{strip} T_y^*(x,y) H_y^{inc}(x,y)\, dx\, dy
\end{aligned}$$

$[V_x]$ and $[V_y]$ are respectively the unknown magnetic voltage expansion coefficients associated with x-directed and y-directed basis function. For the printed slot inside layered waveguide of geometry as shown in Fig. 3, the equivalent TE/TM transmission line model [9], [10] using the immittance approach is as shown in Fig. 4. In Fig. 4, Y_1^{TE}, Y_2^{TE} and Y_3^{TE} are respectively the wave admittances of TE mode in region I, region II, and region III of the waveguide. Similarly, Y_1^{TM}, Y_2^{TM} and Y_3^{TM} are respectively the wave admittances of TM mode in region I, region II, and region III of the waveguide. The admittance looking down from the interface #2 for TE and TM mode are

$$Y_d^{TE} = Y_3^{TE}; \quad Y_d^{TM} = Y_3^{TM} \tag{11}$$

Whereas the equivalent admittance looking up from the interface #2 for the TE and TM mode cases are

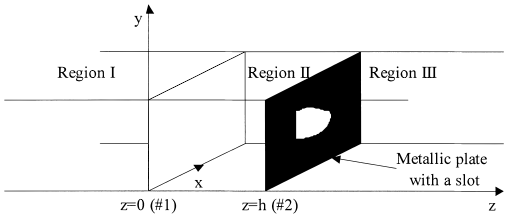

Fig. 3 Geometry of printed slot in layered waveguide.

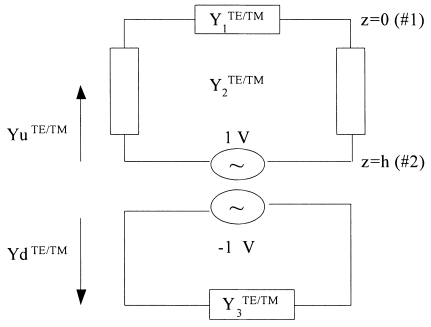

Fig. 4 Equivalent TE/TM transmission line model for transverse magnetic point source excitation in waveguide.

$$Y_n^{TE} = Y_1^{TE}\frac{Y_2^{TE} + jY_1^{TE}\tanh(\gamma_2 h)}{Y_1^{TE} + jY_2^{TE}\tanh(\gamma_2 h)}$$
$$Y_n^{TM} = Y_1^{TM}\frac{Y_2^{TM} + jY_1^{TM}\tanh(\gamma_2 h)}{Y_1^{TM} + jY_2^{TM}\tanh(\gamma_2 h)} \quad (12)$$

In the above equation, γ_2 is the propagation constant of EM wave in the waveguide region II. The magnetic dyadic Green's function in spectral domain when the source and observation points are both at the interface #2 is

$$\begin{aligned}\tilde{\tilde{G}}_{HM}^{22}(\mathbf{k}_t, z = h, z' = h) &= -I_d^{TE}(\mathbf{k}_t, h, h)(\hat{k}_t \times \hat{z})(\hat{k}_t \times \hat{z}) \\ &\quad - I_d^{TM}(\mathbf{k}_t, h, h)(\hat{k}_t)(\hat{k}_t) \\ &= Y_d^{TE}(\hat{k}_t \times \hat{z})(\hat{k}_t \times \hat{z}) + Y_d^{TM}(\hat{k}_t)(\hat{k}_t)\end{aligned} \quad (13)$$

I_d^{TE} and I_d^{TM} denote the current flowing downward from the interface #2 for TE and TM mode respectively. Similarly, the magnetic dyadic Green's function in spectral domain when the source is at the interface #2 and observation point is at the interface #1 is

$$\begin{aligned}\tilde{\tilde{G}}_{HM}^{12}(\mathbf{k}_t, z = 0, z' = h) &= -I_u^{TE}(\mathbf{k}_t, 0, h)(\hat{k}_t \times \hat{z})(\hat{k}_t \times \hat{z}) \\ &\quad - I_u^{TM}(\mathbf{k}_t, 0, h)(\hat{k}_t)(\hat{k}_t) \\ &= -Y_u^{TE}(\hat{k}_t \times \hat{z})(\hat{k}_t \times \hat{z}) - Y_u^{TM}(\hat{k}_t)(\hat{k}_t)\end{aligned} \quad (14)$$

I_u^{TE} and I_u^{TM} denote the current flowing upward from the interface #2 towards interface #1 for TE and TM mode respectively. The above method can be easily extended for any number of layers inside the waveguide and hence the MoM developed can be used for analysis of multiple numbers of printed strips and slots in multi-layered waveguide environment.

2.3 Equivalent Circuit Parameter Extraction

A reciprocal two-port network can be represented by either a T- or π-network as shown in Fig. 5. The elements of a two-port network can be calculated from the transmission matrix by a simple transformation as below:

$$\begin{aligned} Z_a &= (A-1)/C \quad Z_b = (D-1)/C \quad Z_c = 1/C \\ Y_a &= (D-1)/B \quad Y_b = (A-1)/B \quad Y_c = 1/B \end{aligned} \quad (15)$$

The transmission matrix can be obtained from the scattering matrix as follows:

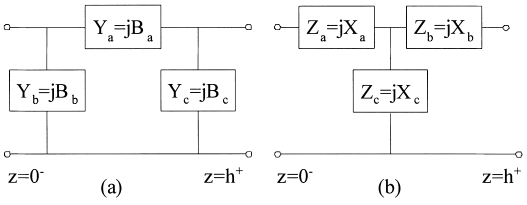

Fig. 5 Equivalent circuit topology (a) π-network (b) T-network.

$$\begin{aligned} A &= ((1+s_{11})(1-s_{22}) + s_{12}s_{21})/2s_{21} \\ B &= Z_0((1+s_{11})(1+s_{22}) - s_{12}s_{21})/2s_{21} \\ C &= (1/Z_0)((1-s_{11})(1-s_{22}) - s_{12}s_{21})/2s_{21} \\ D &= ((1-s_{11})(1+s_{22}) + s_{12}s_{21})/2s_{21} \end{aligned} \quad (16)$$

where Z_0 is the wave impedance of the dominant TE_{10} mode. From the unitary condition of a lossless two-port junction, we have, $s_{22} = -\frac{s_{11}^* s_{12}}{s_{21}^*}$ and for a reciprocal network $s_{12} = s_{21}$. Hence, only two parameters are independent for a reciprocal lossless two-port junction and they can be found by employing the following formulas:

$$\begin{aligned} s_{11} &= E^{scattered}(\mathbf{r})/E^{incident}(\mathbf{r}) \text{ at } z = 0^-, z' = 0^- \\ s_{12} &= E^{scattered}(\mathbf{r})/E^{incident}(\mathbf{r}) \text{ at } z = h^+, z' = 0^- \end{aligned} \quad (17)$$

For lossless networks, the impedance or admittance elements are purely imaginary. Hence, we can get the equivalent circuit parameters from the sign of the impedance or admittance elements.

3. Numerical Results

It has been observed that for obtaining convergent results the slot or strip surface must be divided into at least 10 numbers of meshes. For accurate scattering parameter results, the number of meshes should be chosen as 15 for the dimension of slot or strip equal to the free space wavelength at the frequency under consideration. Figures 6(a) and 6(b) illustrate the convergence plot of S-parameter amplitude and phase for a printed slot of dimension $w = 17$ mm and $l = 3$ mm placed inside a X-band rectangular waveguide ($a = 22.86$ mm and $b = 10.16$ mm) at 17 GHz. The three regions of the waveguide have $\epsilon_1 = 1.0$, $\epsilon_2 = 1.7$, $\epsilon_3 = 1.0$ and h is taken as 1.0 mm. It can be seen that the amplitude of s_{11} starts to converge around 10 numbers of meshes. For the phase of s_{11} parameter the convergent result is obtained when the number of meshes is about 15.

3.1 Numerical Verifications

Let us consider the case of printed strip in a layered waveguide as shown in Fig. 7(a). A rectangular strip of $l = 9.0$ mm and $w = 3.0$ mm is placed at the center of an X-band rectangular waveguide. The three regions as illustrated in Fig. 1 have $\epsilon_1 = 1.0$, $\epsilon_2 = 2.25$, $\epsilon_3 = 1.0$ and h is taken as 1.0 mm. The scattering parameters for a resonant printed strip inside an X-band rectangular waveguide is plotted using the developed EM program and shows good agreement with HFSS results as illustrated in Fig. 8. It has been observed that the printed strip totally reflects the incident wave at the resonance. Next, let us consider the case of printed slot in a layered waveguide as shown in Fig. 7(b). A rectangular slot of $l = 2.7$ mm and $w = 15.5$ mm is placed at the center of an X-band rectangular waveguide. The three regions have $\epsilon_1 = 1.0$, $\epsilon_2 = 2.25$, $\epsilon_3 = 1.0$ and h is taken as 1.0 mm. The scattering parameters for a resonant printed

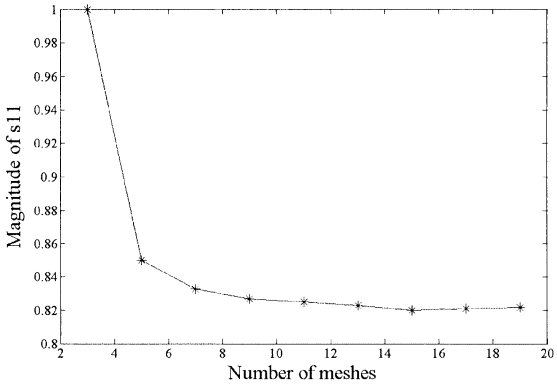

(a)

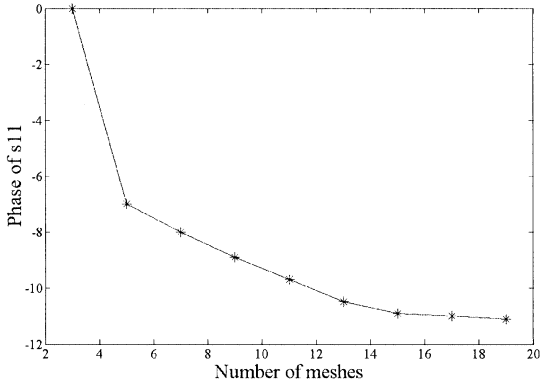

(b)

Fig. 6 Rate of convergence of a printed slot inside a rectangular waveguide (a) amplitude and (b) phase of s_{11}.

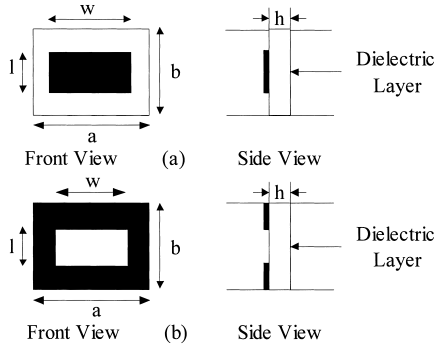

Fig. 7 Geometry of (a) printed rectangular strip (b) printed rectangular slot.

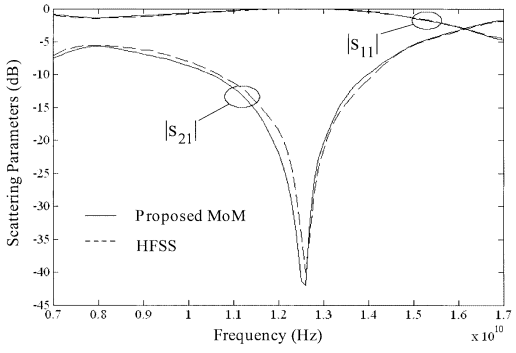

Fig. 8 Scattering parameter for a resonant printed strip in layered waveguide.

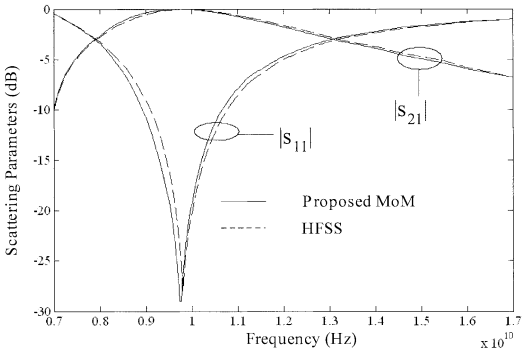

Fig. 9 Scattering parameter for a resonant printed slot in layered waveguide.

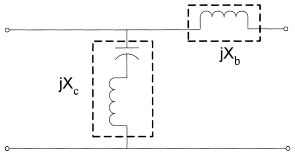

(a)

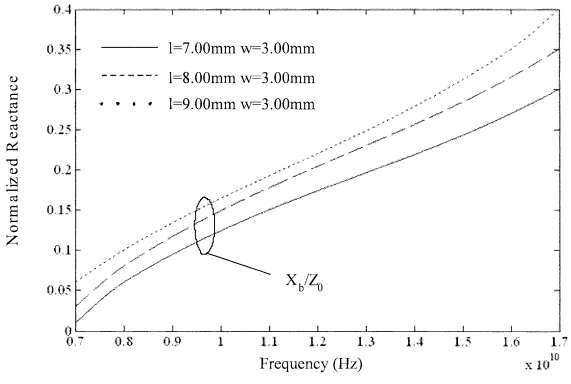

(b)

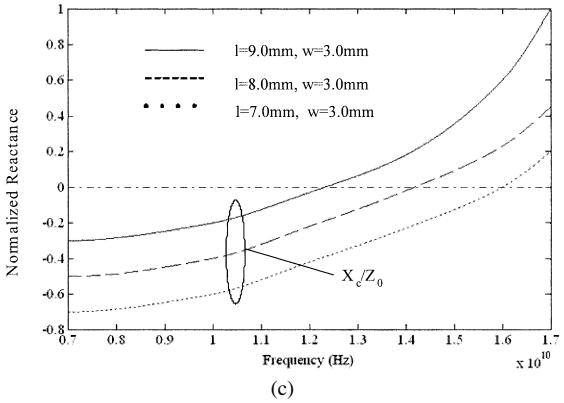

(c)

Fig. 10 (a) Equivalent circuit, (b) Normalized X_b versus frequency and (c) Normalized X_c versus frequency for resonant printed strip in layered waveguide.

slot inside an X-band rectangular waveguide is plotted using the developed EM program and shows good agreement with HFSS results as illustrated in Fig. 9. It has been observed that the printed slot totally transmits the incident wave at the resonance.

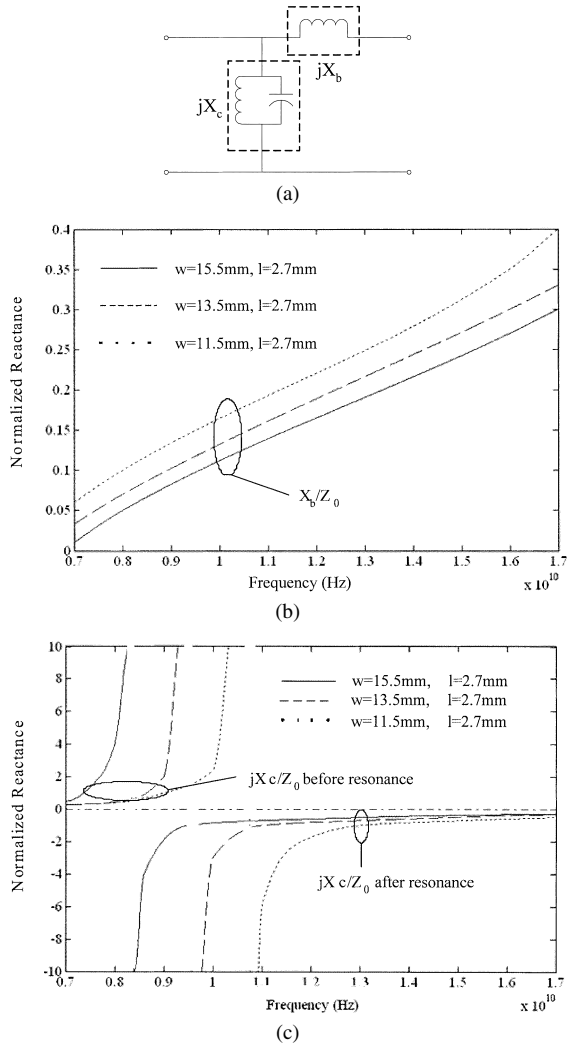

Fig. 11 (a) Equivalent circuit, (b) Normalized X_b versus frequency and (c) Normalized X_c versus frequency for printed slot in layered waveguide.

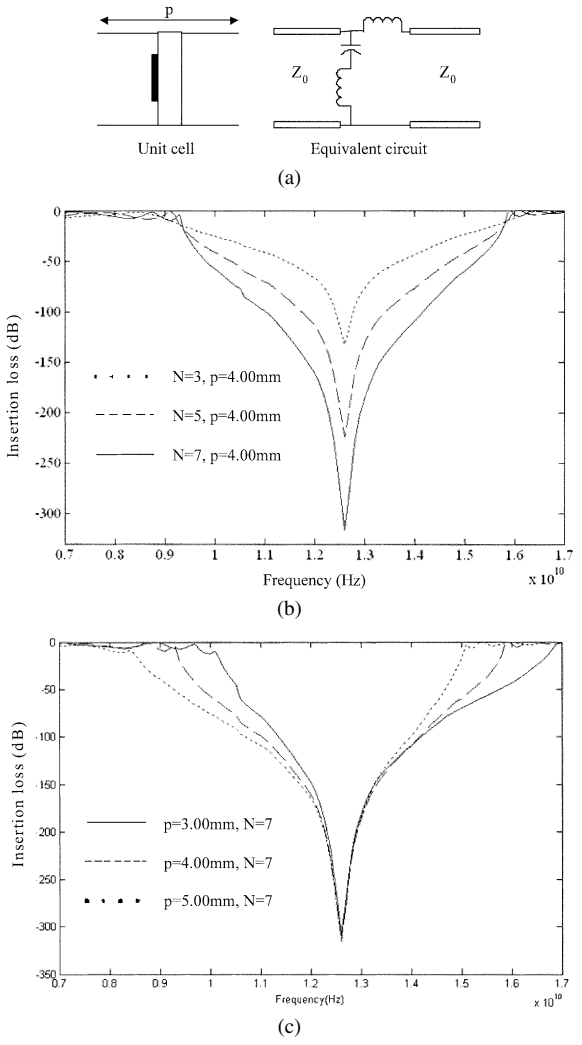

Fig. 12 (a) Geometry and equivalent circuit topology of a unit cell, (b) Insertion loss (s_{21}) of periodic structures with finite number of unit cells $N = 3, 5, 7$ for fixed period $p = 4.00$ mm and (c) Insertion loss (s_{21}) of periodic structures with $N = 7$ for various period $p = 2.0, 4.0, 6.0$ mm.

3.2 Equivalent Circuits

The equivalent circuit of printed strip is shown in Fig. 10(a) and its equivalent circuit parameters in layered waveguide have been extracted following the method described in Sect. 2.3. Figures 10(b) and 10(c) show the variation of normalized X_b and X_c with frequency in the equivalent T-network of Fig. 5(b) for various strip dimensions. From Fig. 10(b) we can infer that the normalized X_b is positive and quasi-linearly increasing with frequency thereby it acts as an inductor. It can be observed from Fig. 10(c) that the normalized X_c is negative at lower frequency region then crosses the zero axis and becomes positive at higher frequency region showing the series resonant behavior. It can be further observed that as we increase the length of the resonant printed strip, the resonant frequency is lowered. Normalized X_a is very small and can be neglected in the equivalent T-network. The equivalent circuit of printed slot is shown in Fig. 11(a). Figures 11(b) and 11(c) show the variation of normalized X_b and X_c with frequency in the equivalent T-network for various slot dimensions. Normalized X_b is positive and increases linearly with frequency as illustrated in Fig. 11(b) hence it acts as an inductor. From Fig. 10(c), we can infer that the normalized X_c is positive in the lower frequency range then goes towards $+\infty$ and suddenly comes down to $-\infty$ around the resonant frequency and becomes negative at the higher frequency range which shows the parallel resonant behavior. We can also observe that the resonant frequency is lowered when the width of the slot is increased. Normalized X_a is also very small and can be neglected in the equivalent T-network.

3.3 Finite Periodic Structures

A finite periodic waveguide structure loaded with units/cells of printed strips of $l = 9.0$ mm and $w = 3.0$ mm and thickness of dielectric layer $h = 1.0$ mm of period p inside an X-

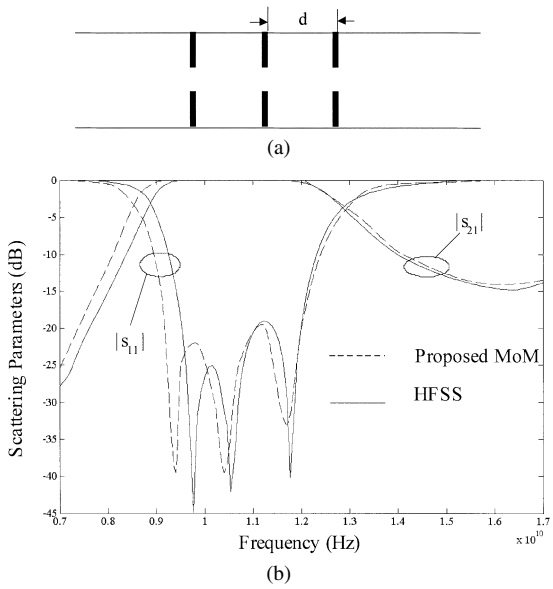

Fig. 13 (a) Geometry of band pass filter, (b) Scattering parameters of the band pass filter versus frequency.

band waveguide has been investigated. The geometry and equivalent circuit topology of the unit cell is illustrated in Fig. 12(a). Figure 12(b) shows the insertion loss (dB) for finite periodic structure with number of unit cells $N = 3$, 5 and 7 for fixed period $p = 4.00$ mm. It can be observed that as the N increases, the insertion loss goes into deep rejection band as mentioned in many literatures like [11]. For $N = 7$, the bandgap or bandstop as defined in [12] is 6.5 GHz for s_{21} below -30 dB at the center frequency of 12.6 GHz which is a very wide bandstop. It has also been observed that there is frequency shift in the electromagnetic bandgap (EBG) as the period of the unit cell changes as illustrated in Fig. 12(c). As the period of unit cell is increased, the EBG of the finite periodic structure shifts to a lower frequency region for a fixed number of unit cells.

3.4 Band Pass Filter

Microwave filters are usually designed for size reduction and/or increased out-of-band rejection [13]. Let us consider a waveguide filter composed of resonant iris i.e. printed slot with no dielectric layer ($h = 0$). A compact and broadband iris filter has been designed based on the simple equivalent transmission line network, in which each parameter is derived using the proposed method. The geometry of the waveguide filter is shown in Fig. 13(a). The distance d between resonant irises is taken as 9.0 mm. The dimension of the iris is $w = 15.5$ mm and $l = 2.7$ mm. The overall ABCD parameter of the filter is obtained by cascading ABCD parameters of every block and is transformed back to scattering parameters to observe the filter performance. The predicted result is compared with those of HFSS as shown in Fig. 13(b) and they are in good agreement. The waveguide filter shows the broadband characteristics with bandwidth = 28.0% for s_{11} below -15 dB at the centre frequency of 10.7 GHz. It takes around 13hrs for the HFSS simulation. But the proposed method takes just several minutes to simulate a single iris then it takes just few seconds to get the performance of the overall filter. Hence the proposed method is more efficient than HFSS specially for designing high-order bandpass filters.

4. Conclusion

A hybrid MoM and immittance approach has been proposed for efficient and accurate analysis of printed strips and slots in layered waveguide. Equivalent circuit parameters are extracted for printed strips and slots in the layered waveguide so that cascaded network based synthesis design can be executed. The method developed is verified in comparison with the results obtained using HFSS and shows good agreement. The proposed MoM will be a very useful tool for various applications like filter design, waveguide synthesis design and full-wave analysis of finite periodic structures.

Acknowledgements

Authors are grateful to Ms Wen Wang and Dr Chao Li for helping with the HFSS simulations.

References

[1] A. Kirilenko and L. Mospan, "Harmonic rejection filters for the dominant and the high waveguide modes based on the slotted strips," IEEE Int. Microwave Symp. Dig., pp.373–376, June 2002.
[2] B.H. Chu and K. Chang, "Analysis of wide transverse inductive metal strips in a rectangular waveguide," IEEE Trans. Microw. Theory Tech., vol.40, no.3, pp.1138–1141, July 1989.
[3] H. Auda and R.F. Harrington, "Inductive posts and diaphragms of arbitrary shape and number in a rectangular waveguide," IEEE Trans. Microw. Theory Tech., vol.32, no.6, pp.606–613, June 1984.
[4] K. Chang and P.J. Khan, "Analysis of a narrow capacitive strip in waveguide," IEEE Trans. Microw. Theory Tech., vol.22, no.5, pp.536–541, May 1974.
[5] G.L. Matthaei, L. Young, and E.M.T. Jones, Microwave Filters, Impedance-Matching Networks, and Coupling Structures, Artech House, Dedham, MA, 1980.
[6] N. Marcuvitz, Waveguide Handbook, MIT Radiation Laboratory Series, vol.10, McGraw-Hill, New York, 1951.
[7] J. Schwinger and D.S. Saxon, Discontinuities in Waveguides, Notes on Lectures by Julian Schwinger, Gordon and Breach Science Publishers, New York, 1968.
[8] A.B. Yakovlev, A.I. Khalil, C.W. Hicks, A. Mortazawi, and M.B. Steer, "The generalized scattering matrix of closely spaced strip and slot layers in waveguide," IEEE Trans. Microw. Theory Tech., vol.48, no.1, pp.126–137, Jan. 2000.
[9] T. Itoh, "Spectral domain immittance approach for dispersion characteristics of generalized printed transmission lines," IEEE Trans. Microw. Theory Tech., vol.28, no.7, pp.733–736, July 1980.
[10] S.-G. Pan and I. Wolff, "Scalarization of dyadic spectral Green's functions and network formalism for three dimensional full-wave analysis of planar lines and antennas," IEEE Trans. Microw. Theory Tech., vol.42, no.11, pp.2118–2127, Nov. 1994.
[11] L. Zhu, "Guided-wave characteristics of periodic coplanar waveguides with inductive loading: Unit length transmission parameters," IEEE Trans. Microw. Theory Tech., vol.51, no.10, pp.2133–2138, Oct. 2003.

[12] R.E. Collin, "Chapter 4: Circuit theory for waveguiding systems'," in Foundations for Microwave Engineering, 2nd ed., McGraw-Hill, New York, 1992.
[13] M. Piloni, R. Ravanelli, and M. Guglielmi, "Resonant aperture filters in rectangular waveguide," IEEE Int. Microwave Symp. Dig., pp.911–914, June 1999.

Rakhesh Singh Kshetrimayum was born in India on February 4, 1978. He received the Bachelor of Technology (first class) degree in Electrical Engineering from the Indian Institute of Technology-Bombay (IITB) in 2000. He is currently working towards his Ph.D. degree in the School of Electrical and Electronic Engineering (EEE) at the Nanyang Technological University (NTU), Singapore. He was awarded IITB MCM Scholarship (1996–2000), KTH-Royal Institute of Technology Electrum Foundation Scholarship (2003–2004) and NTU PhD Research Scholarship (2001–2004). His present research interests include high frequency electronics, spatial power combining, filters, periodic structures and numerical electromagnetics.

Lei Zhu was born on June 19, 1963 in Jiangsu Province, China. He received the B.Eng. and M.Eng. degrees in radio engineering from the Nanjing Institute of Technology (Now: Southeast University), Nanjing, China, in 1985 and 1988, respectively, and the Ph.D. Eng. Degree in electronic engineering from the University of Electro-Communications, Tokyo, Japan, in 1993. From 1993 to 1996, he was a Research Engineer with Matsushita-Kotobuki Electronics Industries Ltd., Tokyo, Japan. From 1996 to 2000, he was a Research Fellow with Ecole Polytechnique de Montréal, Montréal, QC, Canada. Since July 2000, he has been an Associate Professor with the School of EEE, NTU, Singapore. His current research works/interests include the study of planar integrated dual-mode filters, ultra-broad bandpass filters, broad-band interconnects, planar antenna elements/arrays, uniplanar coplanar waveguide (CPW)/coplanar stripline (CPS) circuits, as well as full-wave three-dimensional (3-D) method of moments (MoM) modeling of planar integrated circuits and antennas, numerical deembedding or parameter-extraction techniques, and field-theory-based computer-aided design (CAD) synthesis/optimization design procedures. He is a senior member of IEEE. Currently he is serving as an associate editor of the IEICE Transactions on Electronics and a member of the editorial board of the IEEE Transactions on Microwave Theory and Techniques. He received the Japanese Government (Monbusho) Graduate Fellowship (1989–1993), the First-Order Achievement Award in Science and Technology from the National Education Committee in China in 1993, the 1996 Silver Award of Excellent Invention from the Matsushita-Kotobuki Electronics Industries Ltd., Japan, the 1997 Asia-Pacific Microwave Prize Award presented at the Asia-Pacific Microwave Conference, Hong Kong, and the 2002 JSPS Invitation Fellowship for Research in Japan from the Japan Society for the Promotion of Science.